Acta Crystallographica Section F
Structural Biology and Crystallization Communications
ISSN 1744-3091

Structure of a monomeric variant of rhodopsin kinase at 2.5 Å resolution

John J. G. Tesmer,* Mark R. Nance,‡ Puja Singh‡ and Harie Lee

Life Sciences Institute and the Department of Pharmacology, University of Michigan, 210 Washtenaw Avenue, Ann Arbor, MI 48109-2216, USA

‡ These authors contributed equally.

Correspondence e-mail: tesmerjj@umich.edu

Received 18 August 2011
Accepted 19 April 2012

PDB Reference: GRK1-L166K, 3t8o.

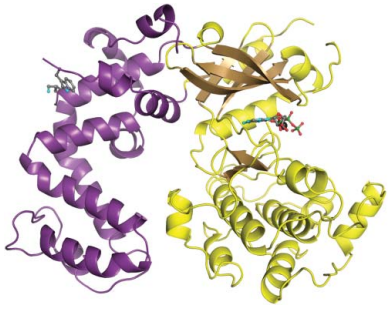

G protein-coupled receptor kinase 1 (GRK1 or rhodopsin kinase) phosphorylates activated rhodopsin and initiates a cascade of events that results in the termination of phototransduction by the receptor. Although GRK1 seems to be a monomer in solution, seven prior crystal structures of GRK1 revealed a similar domain-swapped dimer interface involving the C-terminus of the enzyme. The influence of this interface on the overall conformation of GRK1 is not known. To address this question, the crystalline dimer interface was disrupted with a L166K mutation and the structure of GRK1-L166K was determined in complex with Mg^{2+}·ATP to 2.5 Å resolution. GRK1-L166K crystallized in a novel space group as a monomer and exhibited little overall conformational difference from prior structures of GRK1, although the C-terminal domain-swapped region had reorganized owing to loss of the dimer interface.

1. Introduction

Phosphorylation of activated G-protein-coupled receptors (GPCRs) by GPCR kinases (GRKs) promotes the binding of arrestins, which uncouples the activated receptors from heterotrimeric G proteins (Gurevich *et al.*, 2012). The GRK responsible for the desensitization of rhodopsin in rod cells is rhodopsin kinase (GRK1). Like other GRKs, the catalytic core of GRK1 consists of a Ser/Thr kinase domain inserted into a loop of a regulator of G-protein signaling homology (RH) domain (Tesmer, 2009; Singh *et al.*, 2008; Fig. 1*a*). The region C-terminal to the RH–kinase catalytic core is not conserved among the seven mammalian GRKs (GRK1–7), but is involved in membrane targeting in each case. By interacting with both the large and the small lobes of the kinase domain, the GRK RH domain is thought to stabilize the catalytic core in a conformation that facilitates the rapid phosphorylation of activated GPCRs (Tesmer, 2011; Lodowski *et al.*, 2003).

Previous structural studies of GRK1 demonstrated the formation of a similar RH-domain-mediated homodimer in each of seven different crystal forms (Singh *et al.*, 2008; Huang *et al.*, 2011). The ~2800 Å^2 dimer interface involves hydrophobic residues that are conserved in all GRKs except GRK2 and GRK3 (Fig. 2*a*). A similar crystallographic dimer interface was also observed in the two unique crystal structures of GRK6 (Lodowski *et al.*, 2006; Boguth *et al.*, 2010). In the GRK1 dimer interface only a few C-terminal residues (530–533) are domain-swapped, whereas in one of the GRK6 structures 32 residues are domain-swapped and form extensive interactions with the twofold-related subunit (Boguth *et al.*, 2010). The mutation of conserved residues in the dimer interface, including GRK1-L166K/GRK6-I165E, did not diminish the ability of these enzymes to phosphorylate rhodopsin *in vitro* compared with the wild-type enzyme, nor is there evidence from size-exclusion chromatography that either wild-type GRK1 or GRK6 forms a dimer in solution (Singh *et al.*, 2008; Lodowski *et al.*, 2006). Despite this, dimerization may still occur and be important for other functions *in vivo*.

If the domain-swapped dimer interface is an artifact of a high protein concentration in the crystals, it could influence the overall conformation of the GRK catalytic core and alter the course of the C-terminal residues of the enzyme. To better understand the structure of GRK1 in its monomeric form, we determined the 2.5 Å

Table 1
Crystal and refinement statistics for GRK1-L166K.

Values in parentheses are for the highest resolution shell.

Data-collection details	
Wavelength (Å)	0.99999
Space group	*I*222
Unit-cell parameters (Å)	a = 55.5, b = 149.8, c = 190.9
Temperature (K)	100
Resolution range (Å)	30.0–2.50 (2.59–2.50)
No. of observed reflections	27804 (2732)
Completeness (%)	99.5 (99.0)
Average multiplicity	8.2 (8.1)
$\langle I/\sigma(I)\rangle$	27.9 (2.6)
$R_{\rm merge}$	0.086 (0.792)
Refinement statistics	
No. of atoms/mean B factor (Å^2)	
Protein atoms	3988/26
Mg^{2+}·ATP atoms	32/19
Water atoms and other ligands	59/22
Resolution range (Å)	29.60–2.50 (2.56–2.50)
No. of reflections used in refinement	26394 (1759)
Final overall R factor	0.209
Final $R_{\rm work}$	0.207 (0.334)
No. of reflections for $R_{\rm free}$	1403 (85)
Final $R_{\rm free}$	0.245 (0.406)
Cruickshank DPI† (Å)	0.3
R.m.s. deviations from ideal geometry‡	
Bond lengths (Å)	0.014
Bond angles (°)	1.5
Density correlation coefficient (%)	91.1
MolProbity analysis	
Clashscore	3.8 [99th percentile]
Protein geometry score	1.9 [97th percentile]
Poor rotamers (%)	3.7
C^{β} deviations >0.25 Å	0
Residues with bad bonds (%)	0
Residues with band angles (%)	0
Ramachandran outliers (%)	0
Ramachandran favored (%)	96

† Cruickshank (1999). ‡ Engh & Huber (1991).

resolution crystal structure of the L166K mutant of GRK1 in complex with Mg^{2+}·ATP. The protein crystallizes as a monomer and the overall conformation of the enzyme is not significantly affected compared with prior GRK1 structures. However, the C-terminal domain-swapped region is reorganized owing to loss of the dimer interface.

2. Materials and methods

2.1. Purification of GRK1$_{535}$-His$_6$-L166K (GRK1-L166K)

Bovine GRK1$_{535}$-His$_6$ in pFastBac Dual vector (Singh *et al.*, 2008) was used as a template to generate the L166K mutant using the QuikChange Mutagenesis Kit (Stratagene). Protein expression and purification was carried out as described for GRK1$_{535}$-His$_6$ (Singh *et al.*, 2008) on an Ni–NTA column (Qiagen) followed by Source S chromatography. The peak corresponding to Pool A of GRK1$_{535}$-His$_6$ was used for crystallization. The yield of purified protein varied from 2 to 5 mg per litre of High Five insect cells.

2.2. Crystallization of GRK1-L166K

The L166K variant (8–10 mg ml^{-1}) was cocrystallized in the presence of 4 m*M* ATP pH 7.5 and 2 m*M* $MgCl_2$ by hanging-drop vapor diffusion at 293 K. The well solution consisted of 12% PEG 6000, 100 m*M* sodium citrate pH 4.3 and 5% glycerol. Clusters of rod-like crystals appeared in 2 d and grew to maximum dimensions of 0.3 × 0.02 × 0.01 mm within a week. The crystals were cryoprotected in a solution consisting of 14% PEG 6000, 4 m*M* ATP, 2 m*M* $MgCl_2$, 200 m*M* NaCl, 100 m*M* sodium citrate pH 4.3, 1 m*M* DTT and 25% glycerol.

2.3. Data collection and refinement

Diffraction maxima were collected on a MAR 300 CCD detector on beamline 21-ID-D at the Advanced Photon Source (Argonne National Laboratory). Data were indexed, integrated and reduced using the *HKL*-2000 software package (Otwinowski & Minor, 1997). PDB entry 3c4w (Singh *et al.*, 2008) was used as a search model for molecular replacement in *Phaser* (Storoni *et al.*, 2004) and the model was subjected to maximum-likelihood refinement in *REFMAC*5

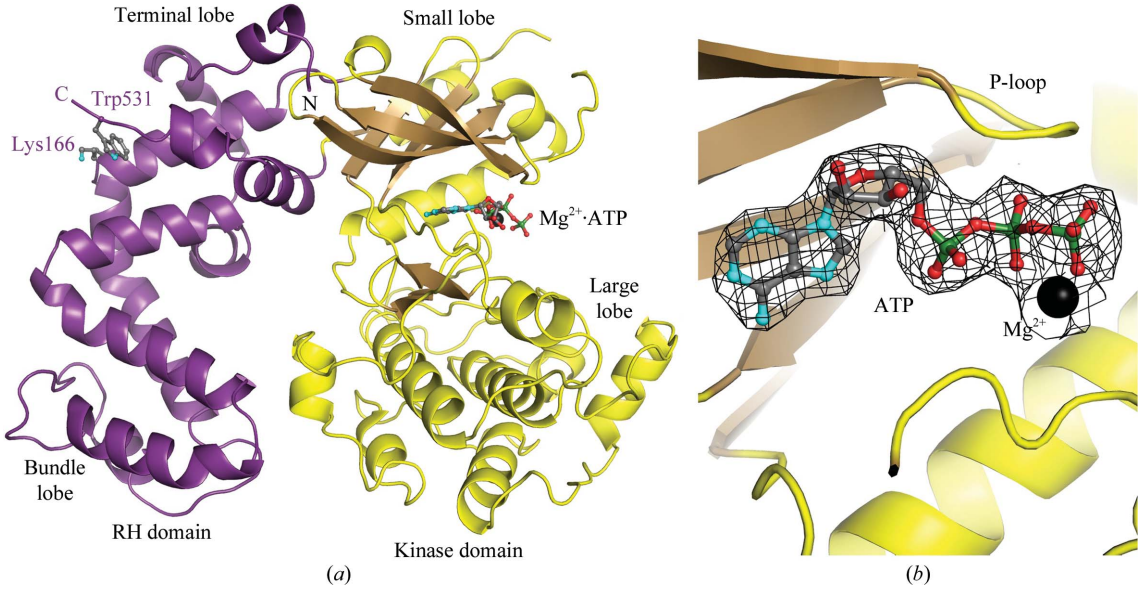

Figure 1
Structure and active site of GRK1-L166K. (*a*) Tertiary structure of GRK1 in a monomeric state. The RH domain is shown in purple and the kinase domain is shown in yellow with brown β-strands. Mg^{2+}·ATP, Lys 166 and Trp531, are shown as ball-and-stick models. in the wild-type enzyme, Leu166 and Trp531 are involved in the dimer interface. The last ordered residues at the N- and C-termini of GRK1-L166K are labeled N and C, respectively. (*b*) Mg^{2+}·ATP bound in the active site of GRK1-L166K. Electron-density from a $2m|F_o| - D|F_c|$ OMIT map generated by excluding Mg^{2+}·ATP is contoured at 1σ as a black wire cage.

(Murshudov *et al.*, 2011) alternating with manual model building using *O* or *Coot* (Emsley & Cowtan, 2004; Jones *et al.*, 1991). The data-collection and refinement statistics are summarized in Table 1. The quality of the refined model was validated with *SFCHECK* (Vaguine *et al.*, 1999) and *MolProbity* (Chen *et al.*, 2010), both of which indicated that the structure is of high quality for its resolution (Table 1), as exemplified by strong OMIT map density for Mg^{2+}·ATP in the active site (Fig. 1*b*). Residues 1–29, 476–480, 488–492 and 533–535 followed by the C-terminal hexahistidine tag were disordered in the structure. Structure-factor amplitudes and coordinates for the GRK1-L66K model have been deposited in the Protein Data Bank (Berman *et al.*, 2000) as entry 3t8o.

3. Results and discussion

3.1. Overall structure of GRK1-L166K

Unlike the previously reported structures of GRK1 and GRK6, GRK1-L166K crystallized as a monomer. Comparison with two prior structures of GRK1 also in complex with Mg^{2+}·ATP (PDB entries 3c4w and 3c4x; Singh *et al.*, 2008) revealed subtle conformational changes within the RH and kinase domains. The RH domain is composed of terminal (residues 30–81, 156–178 and 512–529) and bundle (residues 82–155) lobes (Fig. 1*a*). In the L166K structure, the relative orientation of these lobes differs by 4° from those of the prior structures. The small (residues 179–268 and 495–511) and large (residues 271–466) lobes of the kinase domain (Fig. 1*a*) are likewise rotated by 4° with respect to each other. These two changes are probably coupled because the bundle and large lobes of GRK1 are in contact and their rotations are opposite when viewed along their roughly co-linear rotation axes. Surface loops distant from the dimer interface formed in the wild-type enzyme also adopt novel conformations. For example, the loop that follows the αD helix of the large lobe is poorly ordered in most GRK structures, but has strong electron density and low temperature factors in the GRK1-L166K structure owing to a crystal contact.

The dimer interface observed in prior structures of GRK1 and GRK6 is mediated entirely by the terminal lobe of the RH domain. Superposition of the RH domains of 3c4w and 3c4x with that of GRK1-L166K gives root-mean-squared distances (r.m.s.d.s) of 0.5 and 0.6 Å for 92 and 93 C^{α} atoms, respectively. Omission of residues 50–59 of GRK1-L166K, which have a slightly different conformation and are not part of the dimerization interface, yields r.m.s.d. values of 0.3 and 0.4 Å, respectively. Because the terminal lobes from 3c4w and 3c4x themselves superimpose with an r.m.s.d. of 0.3 Å, loss of dimerization thus does not seem to impose significant conformational changes in the terminal lobe of GRK1 and the observed changes in the relative orientation of the lobes within the kinase and RH domains of GRK1-L166K are more likely to be dictated by differences in crystal-packing environment. Indeed, the observed conformational changes are similar in magnitude to those observed among previously determined structures of GRK1 (Singh *et al.*, 2008).

3.2. Reorganization of the C-terminus of GRK1-L166K

In previous structures of GRK1, the C-terminal residues of the RH domain, beginning at Thr530, cross over the dimerization interface adjacent to the twofold axis to form a short domain swap (Fig. 2*a*). A key feature of this dimer interface is an interdigitated stack of side chains donated by Tyr167, Trp531′, Trp531 and Tyr167′ (where the prime indicates a residue from a twofold-related chain), which in turn

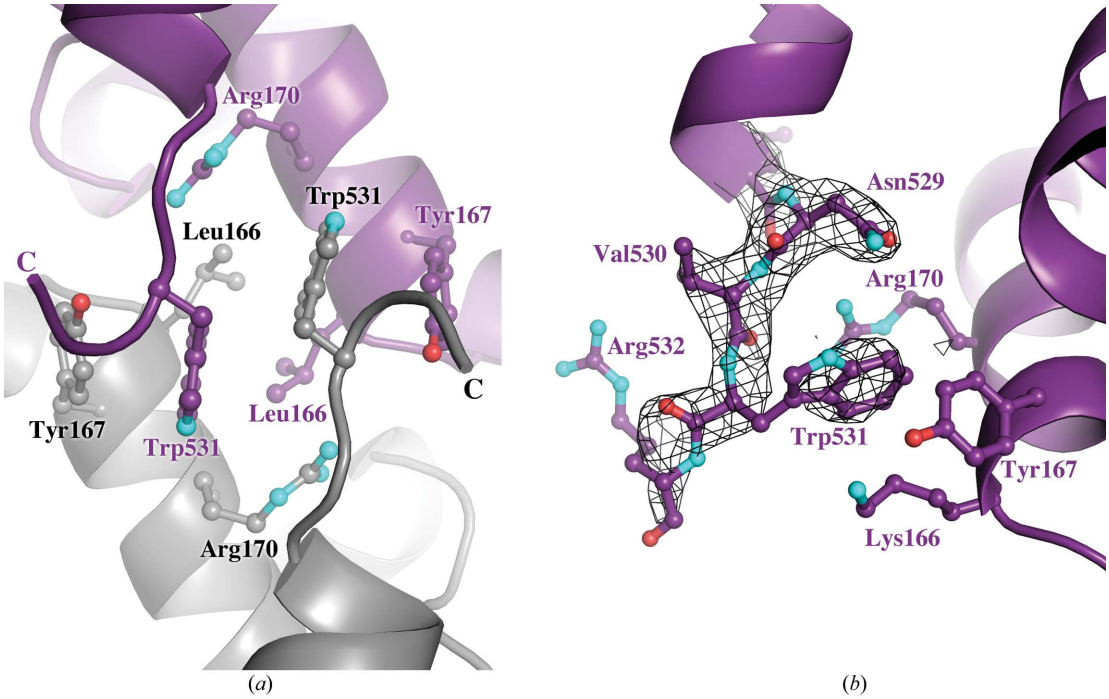

(*a*) (*b*)

Figure 2
Comparison of the dimer interface of wild-type GRK1 that forms in crystals with the analogous region of the L166K mutant in which the interface has been disrupted. (*a*) Structure of the dimer interface in wild-type GRK1, in which the visible region of the C-terminal tail of the enzyme participates in a short domain swap. The side chain of Trp531 from one chain packs in a hydrophobic pocket on the twofold-related subunit formed by the side chains of Leu166, Tyr167 and Arg170. The structure shown is that of PDB entry 3c4w (Singh *et al.*, 2008), with one subunit colored purple and the other gray. (*b*) Structure of the same region in monomeric GRK1-L166K. The side chain of Trp531 now packs between the side chains of Lys166, Tyr167 and Arg170 of its own subunit. A similar packing arrangement is anticipated for wild-type GRK1, with Lys166 replaced by leucine, when it is a monomer. Electron density from a $2m|F_o| - D|F_c|$ OMIT map generated by excluding residues 528–532 is contoured at 1σ as a black wire cage. For clarity, the view is rotated around a vertical axis from that in (*a*).

packs on top of the side chains of Leu166 and Leu166′. Because Leu166 is completely buried at the interface, the L166K mutation was chosen to prevent the formation of a dimer yet retain the aliphatic character of a leucine side chain. In the GRK1-L166K structure the conformation of the last three visible residues, 530–532, is altered in a manner that allows the Trp531 side chain to pack in essentially the same pocket as did the indole ring of Trp531′, where it contacts the side chains of Lys166, Tyr167 and Arg170, although OMIT maps suggest that the indole side chain may not be at full occupancy (Fig. 2*b*). Trp531, Leu166, Tyr167 and Arg170 are highly conserved in GRKs closely related to GRK1 and GRK6, which suggests that the observed structure is not an artifact of the L166K mutation and is indicative of the native structure of GRK1, at least in its monomeric form.

4. Conclusions

The crystal structure of GRK1-L166K is the first of either GRK1 or GRK6 in which the RH-domain-mediated dimer interface is absent. In this state, small structural perturbations occur at the C-terminus that resolve a domain swap imposed by the crystalline dimer interface, yielding a structure that is likely to reflect the configuration of the enzyme in a monomeric state. Although this state is clearly sufficient for the efficient phosphorylation of rhodopsin, dimerization may still be important for other biological processes or interactions that remain to be determined. There is no other large conformational change in GRK1 that can be directly attributed to loss of the dimer interface. Thus, with the exception of the domain-swapped region at the C-terminus, prior crystal structures of GRK1 and GRK6 are likely to exhibit conformations that are not strongly influenced by dimerization of their RH domains.

This work was supported by NIH grants HL071818 and HL086865 (to JJGT). Use of the Advanced Photon Source was supported by the US Department of Energy, Office of Science, Office of Basic Energy Sciences under Contract No. DE-AC02-06CH11357. Use of LS-CAT Sector 21 was supported by the Michigan Economic Development Corporation and the Michigan Technology Tri-Corridor for the support of this research program (Grant 085P1000817).

References

Berman, H. M., Westbrook, J., Feng, Z., Gilliland, G., Bhat, T. N., Weissig, H., Shindyalov, I. N. & Bourne, P. E. (2000). *Nucleic Acids Res.* **28**, 235–242.
Boguth, C. A., Singh, P., Huang, C.-C. & Tesmer, J. J. G. (2010). *EMBO J.* **29**, 3249–3259.
Chen, V. B., Arendall, W. B., Headd, J. J., Keedy, D. A., Immormino, R. M., Kapral, G. J., Murray, L. W., Richardson, J. S. & Richardson, D. C. (2010). *Acta Cryst.* D**66**, 12–21.
Cruickshank, D. W. J. (1999). *Acta Cryst.* D**55**, 583–601.
Emsley, P. & Cowtan, K. (2004). *Acta Cryst.* D**60**, 2126–2132.
Engh, R. A. & Huber, R. (1991). *Acta Cryst.* A**47**, 392–400.
Gurevich, E. V., Tesmer, J. J. G., Mushegian, A. & Gurevich, V. V. (2012). *Pharmacol. Ther.* **133**, 40–69.
Huang, C.-C., Orban, T., Jastrzebska, B., Palczewski, K. & Tesmer, J. J. G. (2011). *Biochemistry*, **50**, 1940–1949.
Jones, T. A., Zou, J.-Y., Cowan, S. W. & Kjeldgaard, M. (1991). *Acta Cryst.* A**47**, 110–119.
Lodowski, D. T., Pitcher, J. A., Capel, W. D., Lefkowitz, R. J. & Tesmer, J. J. G. (2003). *Science*, **300**, 1256–1262.
Lodowski, D. T., Tesmer, V. M., Benovic, J. L. & Tesmer, J. J. G. (2006). *J. Biol. Chem.* **281**, 16785–16793.
Murshudov, G. N., Skubák, P., Lebedev, A. A., Pannu, N. S., Steiner, R. A., Nicholls, R. A., Winn, M. D., Long, F. & Vagin, A. A. (2011). *Acta Cryst.* D**67**, 355–367.
Otwinowski, Z. & Minor, W. (1997). *Methods Enzymol.* **276**, 307–326.
Singh, P., Wang, B., Maeda, T., Palczewski, K. & Tesmer, J. J. G. (2008). *J. Biol. Chem.* **283**, 14053–14062.
Storoni, L. C., McCoy, A. J. & Read, R. J. (2004). *Acta Cryst.* D**60**, 432–438.
Tesmer, J. J. G. (2009). *Prog. Mol. Biol. Transl. Sci.* **86**, 75–113.
Tesmer, J. J. G. (2011). *G Protein-Coupled Receptors: From Structure to Function*, edited by J. Giraldo & J.-P. Pin, pp. 297–315. Cambridge: Royal Society of Chemistry.
Vaguine, A. A., Richelle, J. & Wodak, S. J. (1999). *Acta Cryst.* D**55**, 191–205.